Numerical Simulation of a Controlled-Flow Tunnel for V/STOL Testing

Paresh C. Parikh* and Robert G. Joppa†
University of Washington, Seattle, Washington

A controlled-flow tunnel employs active control of flow through the walls of the wind tunnel so that the model is in approximate free-air conditions during the test. This is achieved by injecting into or extracting from the test section walls the required quantity of air to match the free-air conditions. In the present study, this concept is explored for a three-dimensional jet flapped wing using numerical simulations. An iterative scheme is developed to simulate the working of a controlled-flow tunnel and comparisons are made with other results where available. It is shown that control need be exerted over only part of the tunnel walls to closely approximate free-air flow conditions. The attractiveness of the scheme lies in its ability to provide a low-interference test environment for V/STOL testing.

Nomenclature

AR = aspect ratio
$\{A\}$ = $N \times N$ matrix of model influence coefficients
b = model geometric span
$\{B\}$ = $M \times M$ matrix of tunnel influence coefficients
c = model chord
C_J = jet momentum coefficient
C_L = lift coefficient
H = wind tunnel height
J = jet momentum flux per unit span
M = number of vortex rings describing the tunnel geometry
N = number of vortex elements describing the model
R = radius of curvature of the jet
S = model wing area
U_∞ = freestream velocity
U_t = tangential velocity at bound vortices in the jet
V_N = normal velocity induced by model at a tunnel wall location
$[V_n]$ = N dimensional column matrix of freestream velocity components at model control points
$[V_{FA}]$ = M dimensional column matrix of desired net normal velocity through tunnel control points
$[V_{MT}]$ = M dimensional column matrix representing the effect of the model at tunnel control points
W = wind tunnel width
X = streamwise coordinate with origin at model quarter chord, positive downstream
Y = vertical coordinate, positive upward
Z = lateral coordinate, positive to the right looking downstream
α = model angle of attack
γ = model bound vorticity per unit length
$[\Gamma_m]$ = N dimensional column matrix of model vortex strength
$[\Gamma_T]$ = M dimensional column matrix of tunnel vortex lattice strength
θ = exit angle of the jet measured with respect to the chord

Presented as Paper 84-2152 at the AIAA 2nd Applied Aerodynamics Conference, Seattle, WA, Aug. 21-23, 1984; received Nov. 25, 1984; revision received Nov. 4, 1985.

*Graduate Student (presently, Research Engineer, Vigyan Research Associates, Inc., Hampton, VA). Member AIAA.
†Professor. Member AIAA.

Introduction

WIND tunnel testing of V/STOL models in the very low forward speed—the "transition" regime—poses special problems. A V/STOL model produces high lift by deflecting the incoming air through a large angle. The highly energized vortical wake may impinge on the tunnel floor, resulting in development of flow directed upstream along the floor. As a result, lateral recirculation may develop on the walls and possibly produce erroneous data. In addition, the presence of the wind tunnel walls distort the trajectory of the wake compared to the free-air case, thus makig the accurate simulation difficult.

One of the approaches suggested in the past to deal with these problems has been the construction of the so-called "smart wind tunnels." By special designs, a free-air flowfield (unconfined flow) is produced in such tunnels. Thus, the enclosed model effectively experiences no interference. In the past, these special designs have been achieved by either contouring the wind tunnel walls to make them streamlines of the flow or by adaptive wall concepts.[2,3]

In the present paper, a concept for a "smart" wind tunnel is described for those cases wherein the exterior flowfield can be successfully modeled. The phrase "controlled-flow tunnel" is used for this tunnel, flow through the walls of which is actively controlled during a wind tunnel test. This is achieved by injecting into or extracting from the test section walls the required quantity of air to match free-air conditions.

The Controlled-Flow Tunnel Concept

A basic assumption in the working of a controlled-flow wind tunnel is that potential flow analysis provides an adequate description of the flow far away from the model. In accordance with this assumption, at some distance from the model a fictitious control surface may be constructed. On this control surface potential theory is applicable. Therefore, if at every point on this surface the flow is identical to that of free air, the model inside the control volume will experience no interference.

The principle of operation of a controlled-flow tunnel is schematically shown in Fig. 1. The facility involves combining an on-line computer, the wind tunnel force measurement equipment, and equipment for active flow control through the tunnel walls. The tunnel employs a continuous feedback operational procedure.

Operation of such a tunnel can be described as follows. In advance of the actual wind tunnel test, a computer program is written to represent the model under test. This program uses simple potential flow representation and is capable of calculating the lift of the model in free air and the normal flow at the locations where the tunnel walls would be in an actual test. This enables one to calculate the wall flow as a function of the model lift. This information is stored for use during the wind tunnel test.

During an actual test, the lift on the model is measured for a set of model and tunnel parameters. Based on this value of lift, the required flow through the walls is determined using the precalculated free-air data. This normal flow is then provided using a servomechanism. Because such flow modifications change the lift, a continuous feedback occurs.

It can be seen that a key point in the operation of a controlled-flow tunnel is that the required flow through the walls is precalculated as a function of the measured lift on the model. To do this requires that the potential representation of the model used be able to predict the lift on the model and the induced velocities at far-field points (such as on the tunnel walls) to a reasonable accuracy.

This concept was first studied by Bernstein,[4] who showed analytically and experimentally that the above-mentioned feedback process does converge to free-air results. The model used in his study was a two-dimensional wing. Later, Atkinson[5] extended the concept by means of numerical simulation to a three-dimensional plane wing. An important finding of his study was that only part of the tunnel walls need be actively controlled to get nearly interference-free results. Since both of these studies were carried out on plane wings, the concept was yet to be proven on a real V/STOL system. The present study was, therefore, begun with the objective of extending this concept to a three-dimensional powered-lift system.

A successful completion of the present numerical study requires that each of the steps in the working of an actual controlled-flow tunnel be numerically simulated. This is accomplished in a three-step process. The first of these steps is the development of a potential flow representation of the high-lift system in free air. This is done for a three-dimensional jet flapped wing and results thus obtained are compared with other available data to show the adequacy of the model used. The next step in an actual controlled-flow tunnel is the measurement of lift on the model enclosed in a closed tunnel. In the present analysis, this is done by developing a numerical solution of the "model-in-the-tunnel" problem. The final step in the process is the numerical equivalent of the feedback process and its effect on the model lift. This is achieved by suitably modifying the tunnel wall boundary conditions of the model-in-the-tunnel solution. Results of a study on the effectiveness of partial control are also included.

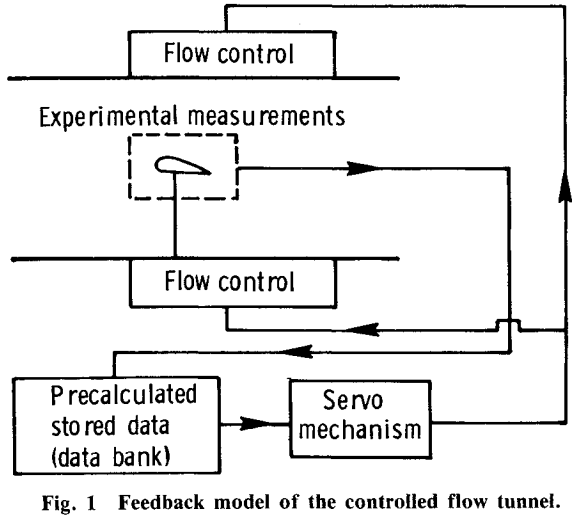

Fig. 1 Feedback model of the controlled flow tunnel.

The Jet Flap Free-Air Solution

A three-dimensional, full-span jet flapped wing was selected for this study, not only because it is the simplest of the many powered-lift systems, but also because aerodynamic characteristics of a jet flap are common to other more practical high-lift systems. One of the first analytical investigations of a jet flap was a two-dimensional theory developed by Spence.[6] Since then, several theories providing more generalities have been presented (e.g., Refs. 7 and 8). A numerical representation suitable for nonlinear, large-deflection cases is given in Ref. 9.

Unlike the conventional plane wing, a jet flap is characterized by a considerably deflected, high-energy jet. The shape of this jet wake is not known a priori and must be determined in any analytical treatment. This wake shape is calculated by iteratively solving for the following two conditions:

1) The kinematic condition of impermeable jet and wing surface,

$$\{A\}[\Gamma_m] + [V_n] = 0 \tag{1}$$

Solution to this equation gives the strengths of the vortices for an assumed location of the jet.

2) The dynamic condition stating that the normal force on the wake is proportional to the jet momentum flux and the local wake curvature,

$$\gamma_m = C_J U_\infty^2 c/2RU_t \tag{2}$$

This changes the trajectory thereby changing the matrix $\{A\}$ and the vector $[V_n]$ and hence an iterative procedure is employed.

The numerical simulation for a three-dimensional jet flapped wing is obtained by suitably modifying Eqs. (1) and (2) to account for the presence of the trailing vortices. Only the salient features are described below in the interest of brevity; interested readers are referred to Ref. 10 for details:

1) An elliptical span loading is assumed. It is represented by an equivalent uniformly loaded wing with a single trailing vortex pair having a vortex span of $\pi/4$ times the geometric span.

2) The jet vortex sheet is represented as a ladder of concentrated bound vortex lines running spanwise and forming a ladder in the streamwise direction. The jet momentum renders the wake "stiff" in the near field and makes spanwise curving negligible. Therefore, the spanwise curvature of these bound vortex lines is only approximately accounted for by taking V-shaped lines.

3) The trailing vortices are taken to be made of short straight vortex segments joined end-to-end in the streamwise direction. The strength of these vortices increases in the streamwise direction to reflect the successive merging of

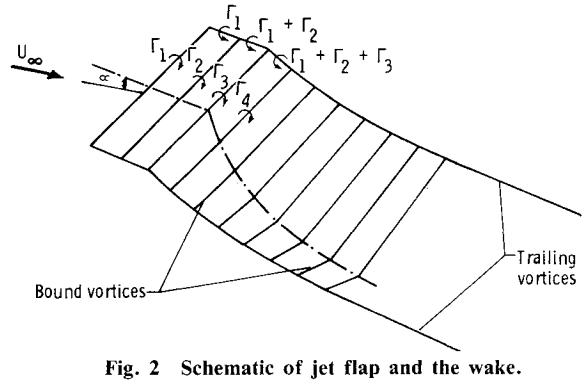

Fig. 2 Schematic of jet flap and the wake.

bound vortices. The correct locations of these vortices are found by making them force-free under the influence of the overall flowfield.

An iterative solution is carried out between the strengths of the bound and the locations of the trailing vortices until a predefined convergence criterion is satisfied. A schematic representation of the jet flapped wing used in the study is shown in Fig. 2.

Computational Results

Extensive comparison of the results obtained using the present analysis was made with other available experimental and theoretical results.[10] Only typical results are presented here. As noted earlier, two key requirements of the free-air representation for the purpose of this work are to calculate lift and far-field-induced velocities to a reasonable accuracy. Comparisons were made with these objectives in mind.

One of the data sources used here for comparison is the classical experiment of Williams and Alexander.[11] These tests were carried out on a rectangular wing of 12.5% thick elliptic section with a full-span jet flap and a jet exit angle of 31.3 deg. The comparison of lift coefficient vs the angle of attack is shown in Fig. 3a. Data obtained from the nonlinear theory of Ref. 9 is also shown. As can be seen, a reasonably good agreement is obtained.

The other set of data used here for comparison was the tests conducted in the University of Washington Aeronautical Laboratory (UWAL) wind tunnel.[12] In these tests, a rectangular full-span jet flapped wing with a span of 3.0 ft and a chord of 0.74 ft was tested in the (8 × 12 ft) test section. The jet exit angle of the wing was 80 deg. The variation of the lift coefficient vs the angle of attack is compared in Fig. 3b and an excellent agreement is obtained. It should be mentioned that in view of the small model-to-tunnel size ratio used in both of these experiments, no wind tunnel wall interference corrections were applied to the experimental data. However, the lift coefficient obtained from the present numerical simulation was corrected for the thickness of the wing as suggested by Spence.[6]

Next, the ability of the present potential flow model to predict the far-field effects, such as the induced velocity at the tunnel wall locations, is checked. In the UWAL experiments, flowfield surveys were conducted to measure the velocity component normal to some fictitious control surfaces. These results are compared with those calculated using the present analysis in Fig. 4 for two locations downstream of the model. Once again an excellent agreement is obtained.

The above results show that the simple flow representation developed here for the three-dimensional jet flapped wing may be adquately used in the analysis.

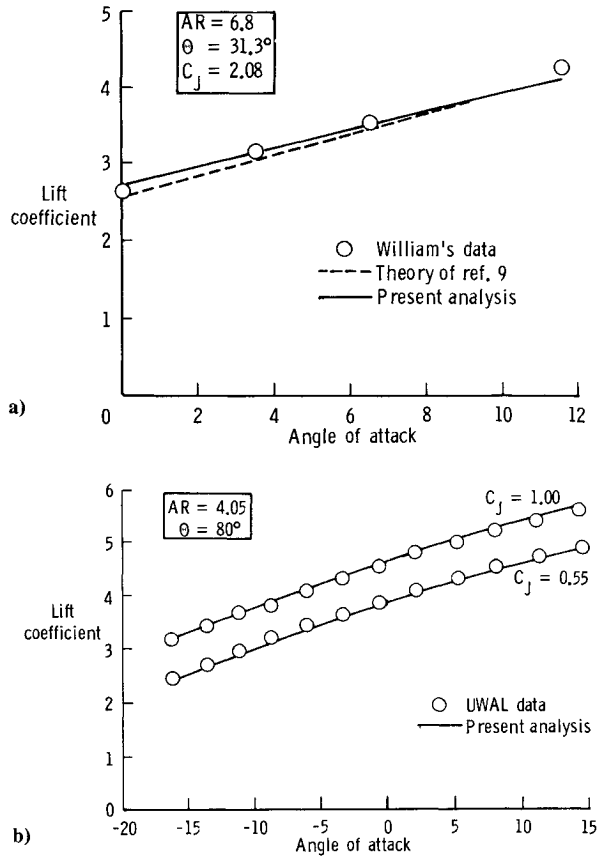

Fig. 3 Comparison of experimental and calculated lift coefficient in free air.

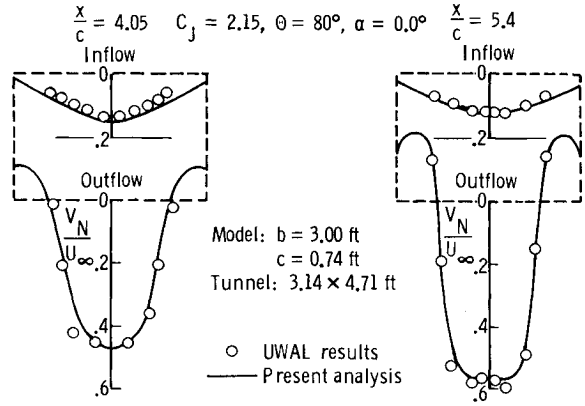

Fig. 4 Distribution of flow normal to control surface.

Model-in-the-Tunnel Solution

One of the steps in an actual controlled flow tunnel involves measurement of lift on a model in a closed tunnel. The numerical equivalent of this requires a suitable representation of the tunnel and a solution of the model-in-the-tunnel problem so that the lift of the model in the presence of the tunnel can be calculated. The solution should also include the vortex wake relocation effect, i.e., accounting for the fact that the wake trails along a different trajectory in the tunnel than in free air. For a plane wing, Joppa[13] has shown that this effect may equal or exceed the wall interference (induced upwash) effect and hence dominate the pitching moment interference.

In the classical interference theory, the effect of the tunnel on the model (the interference effect) is accounted for by using images of the lifting system outside of the tunnel. In an iterative process such as the one described here, the image system has some disadvantages. The curved trailing vortices have curved images. Furthermore, since the shapes of these vortices change from iteration to iteration, so will those of the images. In view of these problems, we use the approach proposed in Ref. 13. In this method, tunnel walls are replaced by a network of vortex lattices. Each vortex rectangle has a circulation strength Γ_T associated with it. The closed-wall boundary condition is satisfied at the center of each rectangle, referred to as the control point. A typical closed-tunnel representation is shown in Fig. 5.

Solution Procedure

The model-in-the-tunnel solution is iterative in nature, accounting for the effect of the tunnel on the model (wake relocation) and the effect of the model on the tunnel in terms of the model-induced velocities at the tunnel control points. The solution proceeds as follows. First, the potential flow solution of the model in free air is obtained as described earlier. Then, the model is enclosed in the tunnel represented using the vortex lattices, and the strengths of these vortices

are found by satisfying the zero normal flow boundary conditions at the tunnel control points. The following matrix notation represents a set of equations, one written for each control point:

$$\{B\}[\Gamma_T] + [V_{MT}] = 0 \tag{3}$$

where the two terms represent the contributions to the normal velocity from the tunnel and the model, respectively. The column matrix $[V_{MT}]$ is calculated knowing the strengths of the vortices representing the model and their location in the tunnel.

Next, the effect of the tunnel on the model is calculated by doing a free-air-like solution using Eqs. (1) and (2), modified appropriately to take into account the presence of the tunnel represented by the vector $[V_{TM}]$,

$$\{A\}[\Gamma_m] + [V_n] + [V_{TM}] = 0 \tag{4}$$

This changes the vector $[V_{MT}]$ and, hence, Eqs. (3) and (4) are solved iteratively until a predetermined convergence is obtained, after which the model aerodynamic coefficients are calculated. The effect of the tunnel is also taken during the wake relaxation process to calculate the relocated wake trajectory.

Results

Computation results obtained using the solution developed here were compared against the UWAL test results.[12] In these tests, results were obtained on a 4.05 aspect ratio full-span jet flapped wing by testing the model in a smaller test section of size (3.14×4.71 ft) inserted in the UWAL (8×12 ft) tunnel. The cross section of the insert was small enough to give a large interference. It may be mentioned that here again the two key requirements of the numerical simulation are to calculate the model lift in the presence of the tunnel and to calculate the correct trajectory of the relocated trailing vortex pair.

Figure 6 shows the variation of lift coefficient of the model in the closed insert vs the angle of attack for two values of the jet momentum coefficient. In the numerical simulation, the tunnel was represented using 280 square vortex rings with 20 rings along the circumference at any cross section of the tunnel. Once again, an excellent agreement is obtained.

The effect of the tunnel in relocating the trailing vortex wake in the tunnel as compared to the free air is shown in Fig. 7. Here, no experimental data were available for comparison, but as expected the upwash due to the presence of the walls resulted in a lesser vertical penetration of the wake.

These results show that the model-in-the-tunnel solution developed here adequately accounts for the effect of the tunnel on the lift of the model and on the vortex wake relocation. This part of the program is the numerical equivalent of an important step in the operation of a practical controlled-flow tunnel—that of measurement of the lift on the model in the tunnel.

Controlled-Flow Tunnel

The final step in the numerical study of a controlled-flow tunnel is the selection of the locations on the tunnel walls to be actively controlled, the amount of control, the mechanical process of the actual control (feedback process), and its effect on the model in the tunnel.

An "ultimate" controlled-flow tunnel would duplicate the flowfield experienced by the model in free air. In such a tunnel, flow would have to be actively controlled from an infinite number of points on all walls. The result of such a process would eliminate all flow distortions caused by the tunnel wall boundaries, resulting in model data requiring no corrections. However, the complexity of the required flow control arrangements would prove to be impractical. These

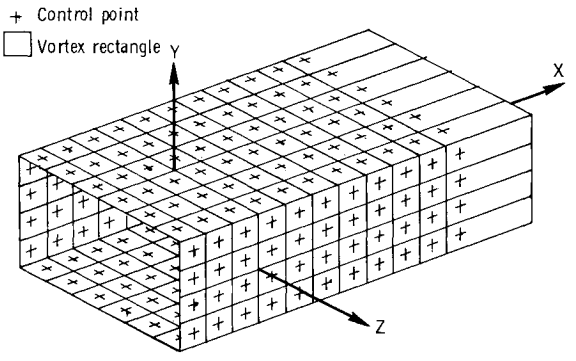

Fig. 5 Representation of a rectangular tunnel by vortex lattice of square vortex rings.

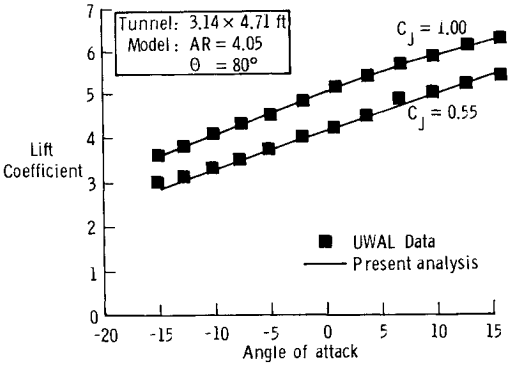

Fig. 6 Comparison of experimental and numerical lift coefficient in uncontrolled tunnel.

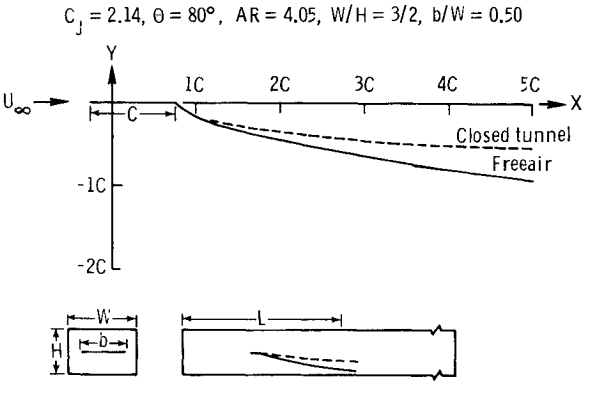

Fig. 7 Vortex wake relocation in uncontrolled tunnel.

arguments prompted Atkinson[5] to study the distribution of free-air normal velocity along those locations where the tunnel walls would be in an actual test. Based on this study, for a plane three-dimensional wing, he found that approximate free-air conditions could be obtained even if the flow through only part of the tunnel walls was actively controlled.

In order to decide the locations to be actively controlled, a similar study was carried out for the jet flap model. Here, the normal velocity induced by the model on the ceiling and floor of an imaginary wind tunnel test section was calculated in free-air flow environment. A typical result is shown in Fig. 8. As can be seen, for the most part, there is flow into the tunnel on the ceiling and out of the tunnel on the floor. On the floor, the magnitude of the normal velocity becomes larger and larger as the wake approaches the floor. Based on such a velocity survey, an effective scheme for defining a limited-activity, controlled-flow tunnel was developed.

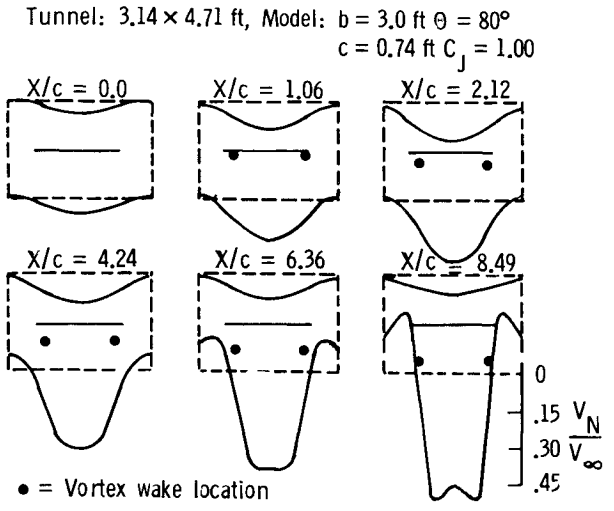

Fig. 8 Free-air normal velocity distribution on the tunnel walls ($\alpha = 0$ deg).

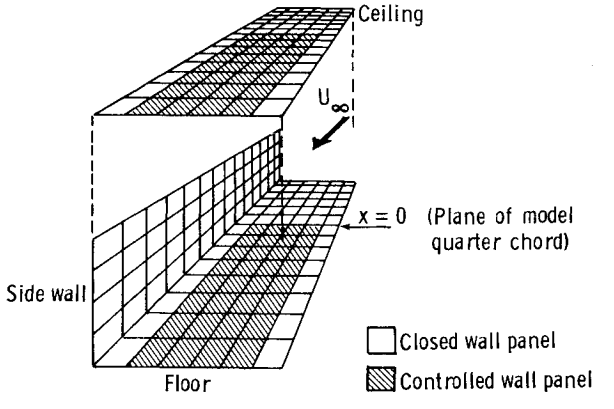

Fig. 9 Control arrangement for partial control.

Numerical Solution

Once the locations for active flow control are determined, the required flow through the tunnel walls would be achieved in a real tunnel by mechanical flow control devices and a new measurement of lift would be made. In the present numerical simulation, the effect of this flow control on the model is calculated by appropriate modifications to the closed tunnel program. These modifications concern the use of correct boundary conditions at the control points on the tunnel walls to represent correct flow velocities in or out of the test section. This is achieved by slight modifications to Eq. (3) to read

$$\{B\}[\Gamma_T] + [V_{MT}] = [V_{FA}] \tag{5}$$

Here, as before, the two terms on the left represent the normal velocity induced at a control point by the tunnel and by the model. The components of the vector $[V_{FA}]$ on the right represent the desired net normal velocity through control points on the tunnel. For an uncontrolled point, this value is, of course, zero and represents a solid segment of the wall. For a controlled wall segment, on the other hand, it is equal to the value the model in the free air would induce at that point.

Solution to this set of equations gives the strengths of tunnel vortex lattices. This is followed by a solution of Eq. (4) to find effect of the flow control on the model wake. As before, repeated iterations are carried out between Eqs. (4) and (5) until convergence is achieved. Also, the effect of the controlled flow on model wake relocation is taken during the wake relaxation process. At the end of this iterative process, the lift coefficient and the wake location are close to their free-air values, depending, of course, upon the amount and distribution of control used.

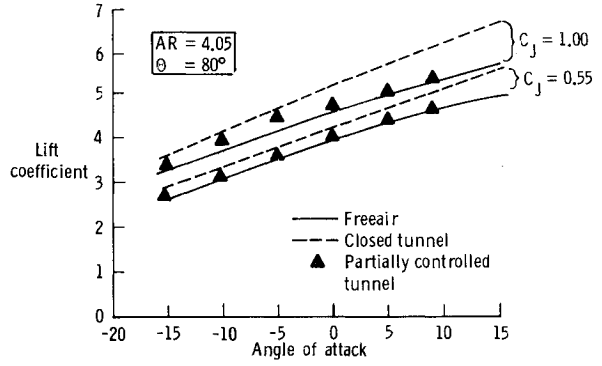

Fig. 10 Variation of computed lift coefficient vs angle of attack for control arrangement of Fig. 9.

Results Using Partially Controlled Tunnel

Based on the above-mentioned normal velocity survey (Fig. 8), it can be seen that if the tunnel is actively controlled on the floor and the ceiling aft of the model quarter-chord line, then a large portion of the free-air flowfield could be reproduced. This was thought to be a good starting point for the study of a partially controlled-flow tunnel. The tunnel for this study was represented using 280 vortex rectangles, of which flow through 64 was actively controlled. The tunnel representation is shown in Fig. 9 and the calculated lift coefficient vs the angle of attack is shown in Fig. 10.

As can be seen from Fig. 10, the control arrangement used is not uniformly successful in restoring the free-air environment over the entire range of angles of attack and jet momentum. This may be the result of the active control being limited to the ceiling and floor only. Thus, a better control arrangement is needed, extending the control over side walls as well.

One such arrangement was obtained by transferring the decision-making process of whether to actively control a particular control point or not to the computer program. Accordingly, a control point on the tunnel was automatically controlled if the magnitude of normal velocity induced by the model at that point was greater than 3% of the freestream velocity. This resulted in 41-57% of the tunnel needing control, depending upon the angle of attack, as opposed to about 22.8% with the previous arrangement. This arrangement produced results almost identical to the free-air ones over the entire angle-of-attack range (Fig. 11). A typical resulting control arrangement is shown in Fig. 12 for the model angle of attack of 0 deg. It can be seen from this figure that, for a high-lift model, active flow control also needs to be extended on the side walls and that on the ceiling and floor it has to be applied over a large area. This is not surprising as the highly deflected wake typical to a high-lift model is closer to the tunnel floor and also because stronger vortices are produced due to the high lift.

It may be mentioned that the distribution of control to be applied over the tunnel walls will depend on many factors, including model-to-tunnel size, location of the model, and its wake relative to walls, etc. These factors can, by no means, be standardized. This is one of the situations where a numerical study such as this is convenient for getting an idea of what is needed even before the actual wind tunnel test begins.

Practical Considerations

The numerical analysis above shows the usefulness of a controlled-flow test section for low-interference results on

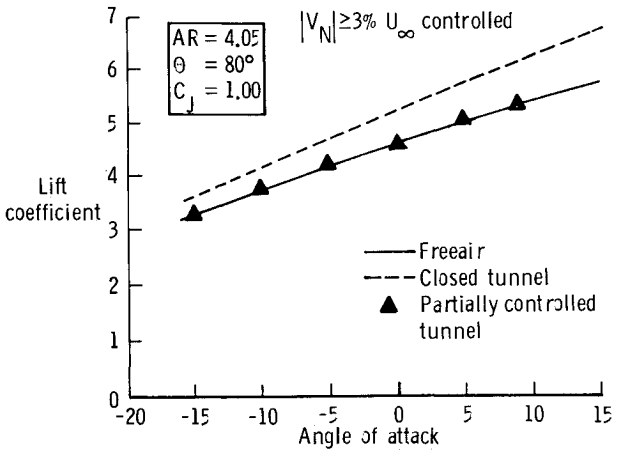

Fig. 11 Comparison of computed lift coefficient showing effectiveness of partial control.

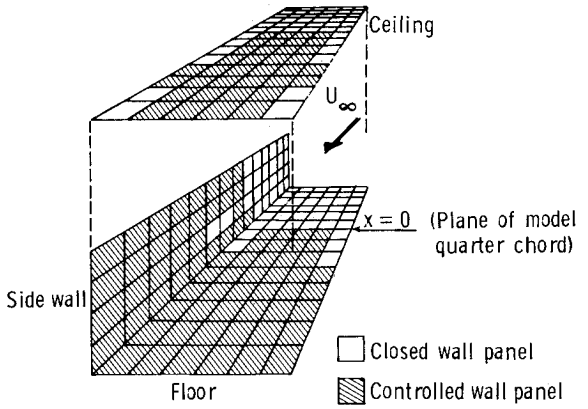

Fig. 12 Typical control arrangement for Fig. 11 ($\alpha = 0$ deg).

high-lift systems. Some operational and other problems that may be encountered during testing in an actual controlled-flow tunnel are mentioned here briefly.

One of the first problems to be dealt with is the development of a potential flow representation for each V/STOL model to be tested. With the introduction of new V/STOL concepts combining jets, rotors, and flow-deflecting devices, simple representation of the models may become difficult. Fortunately, since only an estimate of the gross and far-field effects is demanded by the scheme, advanced vortex lattice computer simulations (e.g., Ref. 14) can be used. Nonlinear mutual interference of various components comprising a V/STOL system can be accounted for in an iterative manner.

In a practical controlled-flow tunnel, air is injected or extracted through discrete holes in the wall so that, if over an area the mass flow is matched to that of the free-air case, its momentum will be greater than ideal. Alternatively, the integral of the momentum of the ideal flow through the surface may be equated to the momentum through the discrete holes, resulting in a mass mismatch.[4] This problem requires a careful study and may be solved only through operational experience.

The entire scheme is iterative and involves feedback and certain aerodynamic lag times that may introduce stability problems in the feedback loop.

Conclusions

The results of this study demonstrate the utility of the concept of the controlled-flow tunnel for low-interference results even in the highly interactive regime of V/STOL models. The potential flow representation used seems adequate for the purpose of this scheme, since it requires only estimates of the gross quantities. The numerical simulation of the controlled-flow tunnel shows that control need be applied over a wider area for a V/STOL model than the simple plane wing studied previously. But the conclusion that only part of the tunnel need be controlled makes the concept more viable economically. In summary, the attractiveness of the concept lies in its ability to provide a low-interference test environment for a variety of V/STOL models without resort to complex analytical treatment.

Acknowledgments

This work was supported by NASA Ames Research Center under Grant NSG 2260. Technical Monitor for the grant was Mr. Victor Corsiglia whose constant encouragement is greatly appreciated. This work formed part of the Ph.D. dissertation for the first author. He would like to thank members of his supervisory committee for guidance.

References

[1]Kroeger, R.A. and Martin, W.A., "The Streamline Matching Technique for V/STOL Wind Tunnel Wall Corrections," AIAA Paper 67-183, 1967.

[2]Sears, W.R., Vidal, R.J., Erickson, J.C. Jr., and Ritter, A., "Interference-Free Wind Tunnel Flows by Adaptive Wall Technology," *Journal of Aircraft*, Vol. 14, Nov. 1977, pp. 1042-1050.

[3]Sears, W.R., "Adaptable Wind Tunnel for Testing of V/STOL Configurations at High Lift," *Journal of Aircraft*, Vol. 20, Nov. 1983, pp. 968-974.

[4]Bernstein, S., "The Minimum Interference Wind Tunnel," Ph.D. Dissertation, Dept. of Aeronautics and Astronautics, University of Washington, Seattle, March 1975.

[5]Atkinson, A.J., "Three Dimensional Low Speed Minimum Interference Wind Tunnel Simulation Based on Potential Modeling," M.S. Thesis, Dept. of Aeronautics and Astronautics, University of Washington, Seattle, 1978.

[6]Spence, D.A., "The Lift Coefficient of a Thin, Jet-Flapped Wing," *Proceedings of the Royal Society of London*, Vol. A238, 1956, pp. 46-68.

[7]Maskell, E.C. and Spence, D.A., "A Theory of the Jet Flap in Three Dimensions," *Proceedings of the Royal Society of London*, Vol. A251, 1959, pp. 407-435.

[8]Kerney, K.P., "An Asymptotic Theory of the High-Aspect-Ratio Jet Flap," Ph.D. Thesis, School of Aeronautical Engineering, Cornell University, Ithaca, NY, 1967.

[9]Addessio, F.L. and Skifstad, J.G., "Theory of an Airfoil Equipped with a Jet Flap Under Low-Speed Flight Conditions," NASA CR-2571, July 1975.

[10]Parikh, P.C., "A Numerical Study of the Controlled Flow Tunnel for a High Lift Model," Ph.D. Dissertation, Dept. of Aeronautics and Astronautics, University of Washington, Seattle, Dec. 1983.

[11]Williams, J. and Alexander, A.J., "Three-Dimensional Wind-Tunnel Tests of a 30 Degree Jet Flap Model," British Advisory Research Council, CP 304, Nov. 1955, pp. 1-49.

[12]Shindo, S. and Joppa, R.G., "An Experimental Investigation of Three Dimensional Low Speed Minimum Interference Wind Tunnel for High Lift Wings," NASA CR-164439, 1980.

[13]Joppa, R.G., "Wind Tunnel Interference Factors for High-Lift Wings in Closed Wind Tunnels," NASA CR-2191, Feb. 1973.

[14]Maskew, B., "A Quadrilateral Vortex Method Applied to Configurations with High Circulation," *Vortex Lattice Utilization*, NASA SP-405, May 1976, pp. 163-186.